Materials Letters 65 (2011) 2121–2123

Contents lists available at ScienceDirect

Materials Letters

journal homepage: www.elsevier.com/locate/matlet

Hydrothermal growth of zirconia nanobars on zirconium oxide

R.A. Espinoza-González [a,*], D.E. Diaz-Droguett [b,1], J.I. Avila [b], C.A. Gonzalez-Fuentes [b], V.M. Fuenzalida [b]

[a] Departamento de Ciencia de los Materiales, FCFM, Universidad de Chile, Av. Tupper 2069, 2° piso, 8370451, Santiago, Chile
[b] Departamento de Física, FCFM, Universidad de Chile, Av. Blanco Encalada 2008, 8370449, Santiago, Chile

ARTICLE INFO

Article history:
Received 5 October 2010
Accepted 16 April 2011
Available online 22 April 2011

Keywords:
Zirconia nanorod
Hydrothermal
Autoclave

ABSTRACT

Zirconia nanorods and nanoparticles were grown hydrothermally starting from zirconium monoxide powder. The process was performed in an autoclave using NaOH as a mineralizer at nominal concentrations 15 M, 20 M and 25 M, and at a temperature of 200 °C for 1 week. The samples were characterized by high resolution transmission electron microscopy, showing that the nanorod diameter spanned from 25 to 200 nm and their length from a few hundred nm up to 2 μm. X-ray photoelectron spectrometry showed that after the treatment all the material was zirconium (IV) oxide, as confirmed by X-ray diffraction and selected area electron diffraction. The latter showed that the nanobars were in the monoclinic phase and the nanopowders in the tetragonal one.

1. Introduction

Zirconium dioxide ZrO_2 (zirconia) is an important ceramic material with applications in solid oxide fuel cells, catalysts, oxygen sensors, damage-resistant optical coatings, as gate dielectric, biomaterial, protective coating for optical mirrors and filters. It is a wideband semiconductor, with bandgap in the range of 5–7 eV, which depends on the phase. The room temperature phase is monoclinic, evolving to tetragonal and cubic with increasing temperature; an orthorhombic form has been reported, too [1]. Nano-sized zirconia has specific optical and electrical properties as well as prospective applications in transparent optical devices, electrochemical capacitor electrodes, oxygen sensors, fuel cells, catalyst and advanced ceramics. It has been recently investigated as an intermediate biomaterial coating [2]. One important area is the coating of solid surfaces with nanostructured zirconia by surface modification which would improve the biocompatibility of ceramic coatings [3].

Cubic zirconia nanotubes 50 nm in diameter and up to 17 μm in length have been deposited electrochemically on zirconium metal using a 1 M $(NH_4)_2SO_4$ electrolyte containing 0.5 wt.% NH_4F in a three electrode cell [4–6]. Using the same electrolyte, but varying the voltage from 10 to 40 V, zirconia nanotubes of 40 nm in diameter and up to 12 μm in length were grown [7]. These nanotubes were orthorhombic when prepared at voltages below 30 V, with some monoclinic material above 50 V. Ti–Zr oxide nanostructures have been recently grown by electrochemical treatment of titanium–zirconium alloys [8].

Electrochemical treatments are limited to substrates of low resistivity. Insulating substrates require other surface modification techniques, such as the hydrothermal process, a process that can be scaled to mass production. Kanade used the hydrothermal treatment to modify the surface of commercial monoclinic zirconia powders of particle size around 500 nm. They used 10 M NaOH solutions in a Teflon container inside an autoclave at 120 °C for 70 h, obtaining spherical particles in the range of 24–36 nm. Their X-ray diffraction (XRD) measurements showed the coexistence of monoclinic and cubic zirconia, and the selected area electron diffraction (SAED) recorded from the nanoparticles showed that they were in the monoclinic phase. They also report on the formation of disordered Zr–Na–O phases [9].

In this paper we report on the hydrothermal treatment of zirconium monoxide ZrO powders at concentrated alkaline conditions, which leads to zirconia nanobars and nanopowder.

2. Experimental

The starting material was commercial ZrO (99.3%, BALZERS). In each experiment three portions of 0.25 g ZrO were put in each of three Teflon vessels, filled with NaOH solutions of 15, 20 and 25 M. The three vessels were placed in an autoclave, sealed and heated up to 200 °C for 7 days. The product was washed with deionized water until neutral pH was achieved, and stored for analysis. The growth parameters were selected based on our previous experience with TiO_2 nanostructures [10,11], which growth requires highly concentrated solutions; and with the growth of zirconate films, which required temperatures around 200 °C and times larger than the titanium based counterparts [12,13].

XRD measurements were performed using Cu Kα radiation (Siemens D5000 diffractometer). Samples for X-ray photoelectron spectrometry measurements (XPS, Physical Electronics 1257 system)

* Corresponding author. Tel.: +56 2 978 4238; fax: +56 2 699 4119.
E-mail address: roespino@ing.uchile.cl (R.A. Espinoza-González).
[1] Present address: Departamento de Física, Facultad de Física, Pontificia Universidad Católica de Chile, Santiago, Chile.

0167-577X/$ – see front matter © 2011 Elsevier B.V. All rights reserved.
doi:10.1016/j.matlet.2011.04.056

were prepared by collecting the powder material on an adhesive tape. Samples for transmission electron microscopy (TEM) and SAED (FEI, Tecnai G2F20 S-Twin) were prepared by ultrasonic dispersion of the powder in isopropanol and putting one drop of the thin slurry on a microscope copper grid.

3. Results

3.1. XRD

XRD measurements performed on the hydrothermally treated samples showed the reflections from monoclinic ZrO_2 in all cases, indicating that the ZrO starting material was oxidized to ZrO_2. No other phases were observed. This means that no crystalline material with Zr–Na–O composition was formed, and that all the starting ZrO material was oxidized to ZrO_2.

3.2. XPS

XPS measurements were performed on the starting as well as on the treated material. The starting ZrO powder, as received, exhibits the XPS 3d photoelectron doublet at 182.4 eV ($3d_{5/2}$) and 184.8 eV ($3d_{3/2}$), energies corresponding to ZrO_2 (spectrum not shown) [14]. The inset (a) of Fig. 1 is a high resolution spectrum of the starting ZrO material after erosion with argon ions. The dominant $3d_{5/2}$ signal is located at 182.4 eV, but the curve fitting shows a second peak at lower binding energy corresponding to a value between the binding energies of metallic zirconium and ZrO_2, attributed to the suboxide ZrO [15]. This means that the surface of the grains is oxidized to ZrO_2. Because of the granular nature of the material, sputtering with argon ions does not fully eliminate this ZrO_2 coating, exposing only a fraction of the bulk ZrO material.

Fig.1b) is a broad scan of a sample treated in 20 M NaOH. A small Na1s photoelectron peak is detected, as shown in the inset c).

3.3. TEM and SAED

The morphological examination by TEM shows three kinds of materials: micrometer sized ZrO_2 grains, ZrO_2 nanobars and ZrO_2 nanopowder.

The TEM observation of powders treated in a solution 20 M NaOH (see Fig. 2), showed the formation of nanobars during the hydrothermal process. They grew on the surface of the precursor particles nearly perpendicular to the surface. The diameter of the nanobars ranged from 20 to 60 nm, and length from 200 to 300 nm. EDS analysis of the nanobars showed a composition of Zr and O, in a ratio Zr:O = 1:2, with no traces of contaminants from the preparation process.

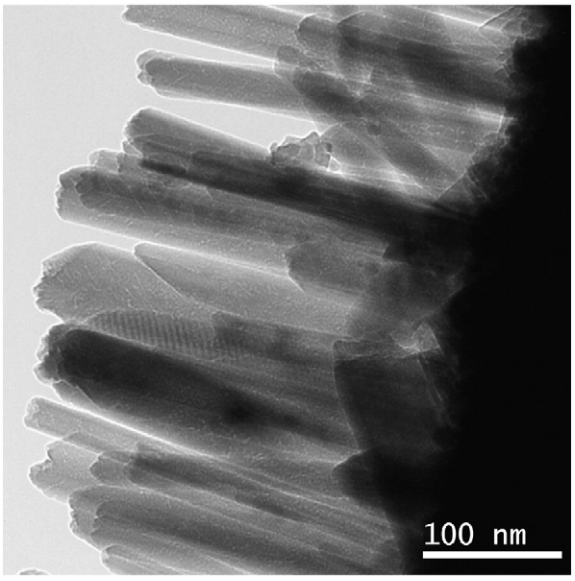

Fig. 2. Bright field image of ZrO_2 nanobars, prepared in 20 M NaOH solution.

Fig. 3 shows nanobars from a sample prepared in a solution 25 M NaOH. The inset is an electron diffraction diagram obtained by Fast Fourier Transform (FFT), showing that the nanobars are in the monoclinic phase. High resolution images allowed the observation that the nanobars tend to growth in [001] direction, as indicated in the figure.

Fig. 4 shows a cumulus of nanoparticles from a sample treated in a solution 20 M NaOH. The inset shows the corresponding diffraction pattern which, opposite to the nanobars, corresponds to the tetragonal phase.

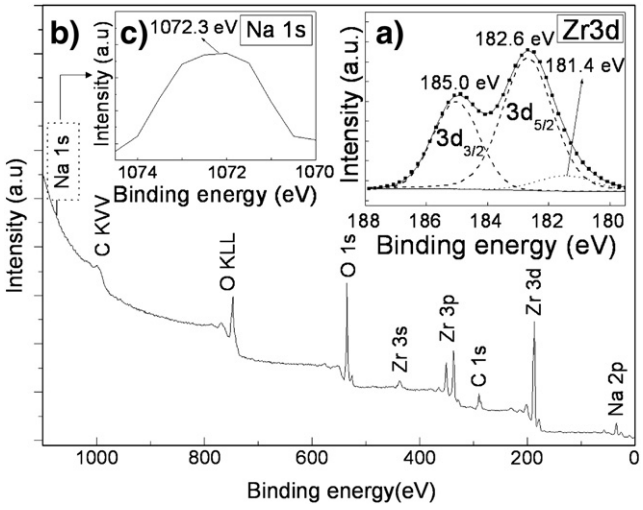

Fig. 1. XPS spectra of zirconium oxide. a) Zr3d doublet from the starting ZrO. b) Broad spectrum from a sample treated hydrothermally and c) zoom showing the incorporation of sodium.

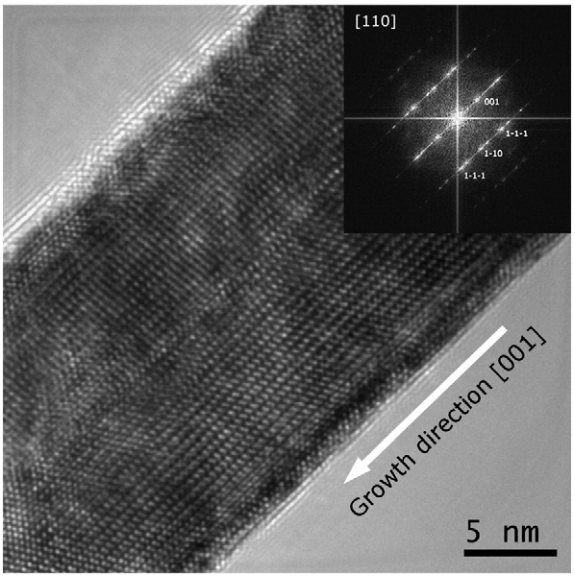

Fig. 3. HRTEM image of zirconia nanobar prepared in 25 M NaOH solution. The inset image corresponds to the FFT, showing the growth direction and a twin along the axis.

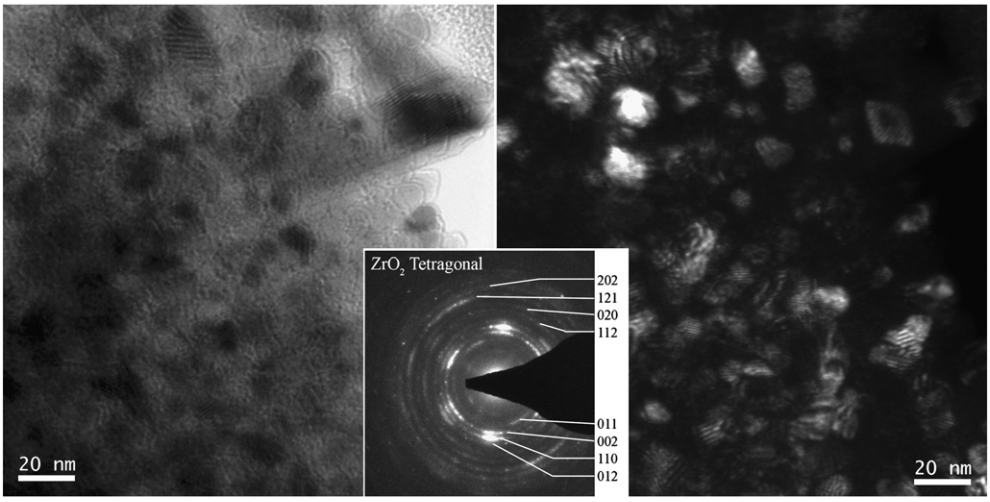

Fig. 4. Bright (left) and dark (right) field images of ZrO_2 nanopowders prepared in 20 M NaOH solution. The inset image corresponds to the diffraction pattern of the cumulous of particles. The dark field image was obtained using the 110 reflection.

4. Discussion

The XRD diagrams showed that all the ZrO starting material was oxidized to ZrO_2. Therefore, the significant differences as compared with the work of Kanade et al. [9] should not be attributed to the different starting material, ZrO or ZrO_2, but to the preparation conditions, i.e. higher temperature, higher mineralizer concentration and longer duration.

XRD did not detect crystalline phases containing sodium, element absent in the nanorods. However, some sodium was detected by XPS, suggesting that these are remnants from the starting solution or that sodium is included in some non-crystalline products as reported in [9], but no sodium is incorporated in the nanorods, which are pure monoclinic ZrO_2. This behavior strongly departs from the growth of titania based nanostructures under similar conditions, which lead to nanowires of sodium–hydrogen titanates instead of pure TiO_2 [10,11].

There is no explanation for the coexistence of two different phases and morphologies. The growth of the monoclinic nanobars can be understood as dissolution followed by reprecipitation, with a growth habit defined by the direction of faster growth. The round nanoparticles can be a remaining of the oxidized starting material after leaching, but this does not explain why they come out to be tetragonal. "No exhaustive theory has been developed to predict quantitatively the formation and growth of nanocrystals with a definite crystal structure as influenced by parameters of a hydrothermal synthesis" [16], and further work must look for the influence of the growth conditions on the overgrowth properties.

The SAED of Fig. 4 corresponds to polycrystalline material, where the reflections are better defined as in samples grown under lower temperatures and shorter treatments (see Fig. 3b of ref. [9]). This means that crystallinity was enhanced by the longer treatment at higher temperature.

5. Conclusions

Large aspect ratio ZrO_2 nanorods grew hydrothermally on ZrO_2 powder particles after hydrothermal treatment in 15, 20 and 25 M NaOH at 200 °C for 1 week. The nanorods were single monoclinic crystals 25 to 200 nm in diameter and a length ranging from a few hundred nm up to 2 μm. No sodium from the solution was incorporated in the nanorods. The nanorods coexist with dispersed ZrO_2 nanoparticles in the tetragonal phase.

Acknowledgments

We acknowledge support from the Chilean Government through grants PSD53 and MECESUP UCH-0205.

References

[1] JCPDS card 791796.
[2] Gu XY, Li X, Liu Q, Chen YX, Li YX YM. Rare Metal Materials Engineering 2009;38(2):1044–6.
[3] Xuanyong Liu, Chu Paul K, Chuanxian Ding. Materials Science Engineering R 2010;70:275–302.
[4] Tsuchiya H, Macak JM, Sieber I, Schmuki P. Small 2005;1:722–5.
[5] Tsuchiya H, Macak JM, Taveira L, Schmuki P. Chem Phys Lett 2005;410:188–91.
[6] Tsuchiya H, Macak J, Ghicov A, Taveira L, Schmuki P. Corrosion Science 2005;47:3324–35.
[7] Zhao J, Xu R, Wang X, Li Y. Corrosion Science 2008;50:1593–7.
[8] Tsuchiya H, Akaki T, Nakata J, Terada D, Tsuji N, Koizumi Y, Minamino Y, Schmuki P, Fujimoto S. Electrochimica Acta 2009;54:5155–62.
[9] Kanade KG, Baeg JO, Apte SK, Prakash TL, Kale BB. Mat Res Bull 2008;43:723–9.
[10] Zarate RA, Fuentes S, Wiff JP, Fuenzalida VM, Cabrera AL. J Physics Chemistry Solids 2007;68:628–37.
[11] Zarate RA, Fuentes S, Cabrera AL, Fuenzalida VM. J Cryst Growth 2008;310:3630–7.
[12] Fuenzalida VM, Pilleux ME. J Mater Res 1995;10:2749–54.
[13] Alvarez Alejandra V, Fuenzalida VM. J Mater Res 1999;14:4136–9.
[14] Moulder JF, Stickle WF, Sobol PE, Bomben KD, Chastain J. Handbook of X-ray photoelectron spectroscopy. 1st ed. Eden Prairie: Perkin-Elmer Corporation, Physical Electronics Division; 1992.
[15] Satoh H, Kawabata S, Nakane H, Adachi H. Surf Sci 1998;400:375–82.
[16] Pozhidaeva OV, Korytkova EN, Romanov DP, Gusarov VV. Russian J General Chemistry 2002;72(6):849–53.